View metadata, citation and similar papers at core.ac.uk
brought to you by CORE
provided by Plymouth Electronic Archive and Research Library

Analysis of the elemental composition of marine litter by field-portable-XRF

Andrew Turner* **& Kevin R. Solman**

School of Geography, Earth and Environmental Sciences
Plymouth University
Drake Circus
Plymouth PL4 8AA
UK

*Corresponding author. Tel: +44 1752 584570; Fax: +44 1752 584710; e-mail: aturner@plymouth.ac.uk

Abstract

Marine litter represents a pervasive environmental problem that poses direct threats to wildlife and habitats. Indirectly, litter can also act as a vehicle for the exposure and bioaccumulation of chemicals that are associated with manufactured or processed solids. In this study, we describe the use of a Niton field-portable-x-ray fluorescence (FP-XRF) spectrometer to determine the content of 17 elements in beached plastics, foams, ropes and painted items. The instrument was used in a 'plastics' mode configured for complex, low density materials, and employed a thickness correction algorithm to account for varying sample depth. Accuracy was evaluated by analysing two reference polyethylene discs and was better than 15% for all elements that had been artificially impregnated into the polymer. Regarding the litter samples, limits of detection for a 120 second counting time varied between the different material categories and among the elements but were generally lowest for plastics and painted items with median concentrations of less than 10 $\mu g\ g^{-1}$ for As, Bi, Br, Cr, Hg, Ni, Pb, Se and Zn. Concentrations returned by the XRF were highly sensitive to the thickness correction applied for certain elements (Ba, Cl, Cr, Cu, Fe, Sb, Ti, Zn) in all matrices tested, indicating that accurate measurement and application of the correct thickness is critical for acquiring reliable results. An independent measure of the elemental content of selected samples by ICP spectrometry following acid digestion returned concentrations that were significantly correlated with those returned by the XRF, and with an overall slope of [XRF]/[ICP] = 0.85. Within the FP-XRF operating conditions, Cl, Cr, Fe, Ti and Zn were detected in more than 50% and Hg and Se in less than 1% of the 367 litter samples analysed. Significant from an environmental perspective were concentrations of the hazardous elements, Cd, Br and Pb, that exceeded several thousand $\mu g\ g^{-1}$ in many cases.

Keywords: marine litter; XRF; plastics; ropes; foams; metals

1. Introduction

The accumulation of marine litter in the open ocean and on beaches is a significant and pervasive global problem. Discarded solid waste has a multitude of both land-based and marine-based sources and arises through a lack of awareness and poor or ineffective waste management practices. As well as representing an aesthetic problem on the foreshore and a nuisance to boaters, manufactured or processed items of waste that are composed of persistent, durable and low-density materials, like plastics, rubbers and ropes, pose serious threats to wildlife through ingestion, suffocation and entanglement [1]. Ingestion of small fragments of litter also affords a route of exposure to and accumulation of chemicals that are associated with these materials [2]. Such chemicals are either an inherent component or degradation product of the solid itself, or may have accumulated from sea water during suspension and transportation of the litter [3].

Although hydrophobic organic pollutants, including polychlorinated biphenyls and polycyclic aromatic hydrocarbons, have been well-studied in this respect [4-6], recent attention has also focussed on the association of various trace metals, like Cd, Cu, Cr, Ni, Pb and Zn, with plastic litter. Thus, controlled laboratory experiments have shown that small quantities of metal can rapidly adsorb onto the plastic surface from sea water [7] while mild acid digestion of beached plastics has revealed that greater quantities of metals can gradually accumulate in natural films coating the polymer [8]. More important from a bulk concentration perspective, however, is the association of certain metals with plastics and other synthetic solids arising from the manufacturing process itself [9]. For example, many metals and metalloids and their compounds are used, or have been used before restrictions came into place, as colourants, fillers,

stabilisers, catalysts, biocides and flame retardants and at concentrations of up to several per cent on a dry weight basis [10]. While most additives are designed to be non-migratable from the virgin matrix, leaching may be facilitated by ageing and abrasion of the solid [9], or the very conditions that marine litter are subjected to during transport in sea water and subsequent beaching.

The analysis of metals in manufactured and processed solids by wet chemical means, involving the complete digestion of the material in concentrated acid and subsequent analysis by, for example, inductively coupled plasma (ICP), spectrometry is rather time-consuming and labour-intensive. More appropriate for the analysis of beach litter, therefore, is a non-destructive technique that allows the rapid throughout of samples of diverse composition and that can be used to explore the spatial distribution of metals within a single- or multiple-component sample. With the miniaturisation of x-ray sources, reduction in battery power requirements, and improvements in detector resolution, detection limits, precision and standardless calibrations, field-portable-x-ray fluorescence (FP-XRF) spectrometry meets these needs [11].

Nakashima et al. [9] recently employed energy dispersive FP-XRF spectrometry (alpha-6500, Innov-X) to determine the concentrations of five metals-metalloids (As, Cr, Pb, Sb, Sn) in a number of plastic items retrieved from a beach in south west Japan. Measurements were corrected using element-specific and material-specific regression equations that related XRF measurements to those returned by ICP after HNO_3-H_2SO_4 digestion. Unfortunately, however, data reported in the article were limited to mean concentrations of Pb in polyethylene, polypropylene and polyvinyl chloride (PVC) and a mean concentration of Sn in PVC. Moreover, little information

was provided on the XRF methodology itself, including counting time, fluorescent x-ray energy ranges, potential interferences, thickness considerations, and the mode and internal calibration of the instrument.

In the present paper, we describe the use of a Niton FP-XRF spectrometer to determine the concentration of a larger suite of elements (n = 17) in a wide variety of samples of marine litter (including plastics, rubbers, expanded-extruded materials, processed corks, ropes, netting and painted surfaces) retrieved from four different beaches. We use the instrument in a 'plastics' mode that is specifically configured for the analysis of complex, low density materials, and evaluate the effects of sample thickness, density and heterogeneity and various aspects of quality control, including a comparison with independent ICP measurements based on analysis of acid digests. The advantages and limitations of the XRF technique used both in situ and ex situ are also discussed.

2. Materials and methods

2.1. Sampling and sample locations

Four beaches in south west England were visited just after high water on single occasions between late August and late September, 2015. Saltram beach is a small, sandy, intertidal region on the east bank of a shallow, urbanised estuary (Plym) that is close to a recently capped landfill site. Mount Batten is a south-facing pebble-sand beach in Plymouth Sound, a bay that receives freshwater inputs from the Plym and Tamar estuaries and, being protected to the south by a 1.6 km breakwater, is a natural harbour for naval and commercial ships and a popular location for yachting.

Constantine Bay and Porth Kidney are sandy beaches on the north (Atlantic) coast of Cornwall and are popular destinations for both tourists and surfers.

On each beach, visible pieces of litter were collected by hand from a transect of the high (or highest) water line. The length of each transect varied between about 10 m and 200 m depending on the abundance of material (and ensuring that at least 50 samples were collected in each case). Litter retrieved included whole objects and fragments of plastic and rubber, pieces of low density expanded-extruded plastic and rubber and fragments of processed cork (the latter being visually very similar to many expanded polymers), offcuts of rope, fabric and netting, and painted wood, fibreglass and synthetic resin; hereafter, these components are classified as plastics, foams, ropes and painted surfaces, respectively. Note that litter not considered in the present study included metal objects, pieces of glass, paper items, unpainted wood and films of food packaging that appeared to have been recently discarded in situ.

Litter from each beach was stored in a series of clear polyethylene bags and transported to the laboratory where individual items were cleared of sand and other debris under running tap water and with the aid of a Nylon brush before being dried at 40 ^{o}C in an oven for 12 h or, for foams, under desiccation at room temperature for up to 96 h. Samples were then weighed on a five-figure balance and stored individually in labelled polyethylene specimen bags and in the dark pending analysis.

2.2. XRF analysis

Samples of litter were analysed by energy dispersive FP-XRF using a battery-powered, field portable (1.3 kg) Niton XRF analyser (model XL3t 950 He GOLDD+).

The instrument employs a miniature, low power x-ray tube with an Ag transmission anode operating at up to 50 kV of high voltage and 200 μA of current as the source of sample excitation, and is fitted with a geometrically optimised large area silicon drift detector to detect and register characteristic x-rays from the sample. The concentrations of As, Ba, Bi, Br, Cd, Cl, Cr, Cu, Fe, Hg, Ni, Pb, Sb, Se, Sn, Ti and Zn, whose fluorescent peaks range from 2.62 keV (Cl-K_α) to 32 keV (Ba-K_α), were determined in a plastics mode through a fundamental parameters-based alpha coefficient correction model. This iterative approach accounts for background matrix effects by describing measured fluorescent x-ray intensities using mathematical equations that tie together the physics of the interaction of x-rays with sample components [12]. Fundamental parameters eliminates the requirement for sample-specific standards, has a wide dynamic range and is independent of the size and shape of the surface [11].

Because polymers are composed of light elements, and primarily carbon and hydrogen, they are weak absorbers of x-rays, and below a critical, saturation thickness, d_{sat}, the measured intensity of x-rays will be dependent on both the analyte concentration and the thickness of the sample, d. For polyethylene, d_{sat}, is about 9 mm, while for polyvinyl chloride (PVC) the abundance of chloride results in a d_{sat} of about 5 mm. For polymers containing heavier elements as, for example, contaminants and additives, d_{sat} is reduced compared with that of the pure material, while in expanded-extruded synthetic polymers, ropes and corks, the presence of air results in densities that are reduced compared with those of the corresponding unexpanded or air-free equivalents and d_{sat} is increased. For the analysis of polymeric materials in the plastics mode, the Niton XL3t 950 GOLDD+ has a thickness correction algorithm

down to 0.05 mm that employs a compensation for mass absorption coefficient based on Compton scatter so that variations in density are factored in. In practice, the thickness of each sample needs to be measured (in mm) before being analysed and if it falls below d_{sat}, the corrective algorithm should be applied with the appropriate (measured) thickness.

In the present study, thickness correction was employed for all plastic samples of $d <$ 10 mm, including those identified by the XRF as PVC (based on Cl content), and to expanded-extruded polymers, ropes and corks of $d < 100$ mm (effectively all samples in these categories). Thickness itself was determined through the flattest ('measurement') surface using 300 mm Allendale digital callipers, and to increase the effective depth and flatness of thin or hollow samples, items were often cut (with scissors, pliers or a blade), folded or layered and, where necessary, held in place using crocodile clips. Regarding the painted surfaces, a thickness correction of 0.05 mm was applied in order to ensure that measurements were made of the surface film while minimising interferences from the underlying wooden or polymeric substrates.

The XRF was used in the laboratory in a bench top accessory stand (with the nose upwards) and was connected to a laptop computer via USB and a remote trigger. Samples were placed on to a SpectraCertified Mylar polyester 3.6 μm film with the measurement surface facing downwards. The slide was then positioned such that the sample lay directly and centrally over a 3 mm small-spot collimator above the 8 mm XRF measurement window, a process aided by referring to real-time video footage generated by an integrated CCD camera adjacent to the detector. On closing the steel shield of the stand, measurements with appropriate thickness correction were

activated through the laptop for a total period of 120 seconds; specifically, counting was performed for 60 seconds each in a low energy range (20 kV and 100 μA: Cl, Cr and Ti) and main energy range (50 kV and 40 μA: all remaining elements). Spectra were quantified by fundamental parameter coefficients to yield elemental concentrations on a dry weight basis (in $\mu g\ g^{-1}$) and with a counting error of 2σ (95% confidence). At the end of each 2-6 h sample measurement session, spectra and elemental concentrations were downloaded to the laptop using Niton data transfer (NDT) PC software.

2.3. Sample digestion and analysis by ICP

As an independent and more sensitive measure of the elemental content of marine litter, a variety of samples (n = 18), encompassing all material categories with the exception of painted surfaces and that had already been tested by XRF, were digested in Fisher Scientific TraceMetal grade acids (and ammonia) and analysed by inductively coupled plasma-optical emission spectroscopy (ICP-OES). Thus, offcuts or slices of plastic, foam (including cork) and rope of between about 50 mg and 200 mg were prepared with a stainless steel blade before being accurately weighed into individual 100 ml borosilicate Tecator tubes. Three ml of concentrated sulphuric acid was added to each tube and the contents heated to 300ºC for about 2 h in an aluminium digestion block. To the resulting digests, concentrated HNO_3 was carefully added dropwise until the solutions changed from black to pale yellow or colourless. After the covered contents had been allowed to cool overnight, digests were transferred to 50 ml glass volumetric flasks and diluted to mark with 2% HNO_3. To any digests containing a visible precipitate (presumably $PbSO_4$ and/or $BaSO_4$),

concentrated ammonia solution was added dropwise until the solids cleared. Procedural controls were undertaken likewise but in the absence of litter samples.

Digests were analysed for all elements detected by XRF and that were measurable by ICP-OES (thereby excluding Cl and Br) using a Thermoscientific iCAP 7400. The instrument was calibrated using four mixed standards and a blank prepared by serial dilution of CPI International standards in 2% HNO_3, and settings in both UV and visible light were as follows: exposure time = 2 s; RF power = 1150 W; nebuliser, coolant and auxiliary gas flows = 0.50, 12 and 0.5 L min^{-1}, respectively; viewing height = 12 mm; uptake time = 50 s; wash time = 15 s.

2.4. FTIR analysis

In order to identify the component polymers in the plastics, foams and ropes, selected samples (n = 50) were analysed by attenuated total reflection-Fourier transform infra-red spectroscopy (ATR-FTIR) using a Bruker ALPHA Platinum ATR QuickSnap A220/D-01 spectrometer. Samples were cut to a suitable size, where necessary, using a stainless steel scalpel, and then firmly clamped down on to the ATR diamond crystal in order to ensure good contact and sufficient penetration of the evanescent wave. Measurements, consisting of 16 scans in the range 4000 to 400 cm^{-1} and at a resolution of 4 cm^{-1}, were activated via Bruker OPUS spectroscopic software, with subsequent identification involving comparisons of transmittance spectra with libraries of reference spectra.

3. Results and Discussion

3.1. Sample characteristics

A total of 376 litter samples retrieved from four beaches of south west England were analysed in the present study, of which 149 were categorised as plastics, 149 as foams (including processed corks), 68 as ropes and 10 as painted surfaces. The mass of individual items of plastic ranged from less than 10 mg for various unidentifiable fragments to over 10 g for relatively large fragments and specific objects (e.g. toys, a bodyboard clip and a cigarette lighter); thickness through the flattest surface, *d*, ranged from about 0.3 mm for several flexible films after folding or stacking to more than 10 mm for many of the largest fragments and objects. The mass of the foams ranged from less than 3 mg to 50 g and *d* ranged from about 0.5 to 40 mm, with most items being fragments of various size, shape and colour (but mainly off-white or yellow-brown). The mass of ropes ranged from about 20 mg for a small fragment of fabric to over 40 g for a multi-coloured offcut of rigging, with *d*, after any deliberate intertwining of fishing line or frayed netting, ranging from about 2 to 12 mm. The mass of painted surfaces ranged from about 1.7 to 150 g, with the bulk of the material representing the underlying substrate, and in all cases *d* (of the surface) was assumed to be 0.05 mm (see above).

FTIR analysis of selected samples revealed that plastic items and fragments were mainly polyethylene or polypropylene but a few were polyvinyl chloride (PVC), and that offcuts of rope and netting were generally polyethylene or polypropylene but fishing lines were Nylon. Many pieces of expanded-extruded polymer could not be identified definitively but those yielding clear spectra were predominantly polystyrene or polyurethane with some fragments composed of elasticated rubber, PVC, rayon or acrylic. Because information on cork was not contained in the reference libraries, such

samples were verified by comparisons of spectra with those derived from direct measurements of a series of cork stoppers.

3.2. Detection limits

FP-XRF is able to detect elements that elicit a sufficiently strong fluorescence signal relative to background intensity that is free from interferences arising from the matrix and from the interactions of other elements (peak overlaps and absorption and enhancement effects). The limit of detection (LOD) is, therefore, dependent on the element (or its x-ray activity and the energies of its fluorescence peaks), detector resolution, mode of application of the instrument, counting time, sample thickness, physical and chemical composition of the material, and statistical criteria used for defining detection. The Niton XLT3t series of analysers define LODs that are specific to the characteristics of the sample and the counting time as three standard deviations ($1.5 \times 2\sigma$, or 99.7% confidence interval), and measurements are reported in the NDT output only where concentrations exceed this threshold with calculated detection limits provided otherwise. The lower LODs specified by the manufacturer for elements in 'clean' polymers of unspecified thickness that are relatively free of inter-element spectral interferences and for a 30-second total counting time in plastics mode range from less than 10 $\mu g\ g^{-1}$ (As, Bi, Br, Hg, Pb and Se) to 100 $\mu g\ g^{-1}$ (Ba) in polyethylene and from less than 20 $\mu g\ g^{-1}$ (As, Br, Cd and Pb) to more than 100 $\mu g\ g^{-1}$ (Fe) in PVC.

LODs based on the analysis of the more varied and complex litter samples are shown in Table 1. Here, the median, minimum and maximum calculated limits for each element and for each category of sample are provided for a total counting time of 120

seconds and with appropriate thickness correction where applicable (see below), along with the numbers and percentages of samples that were not detected in each case. Within a specific material category, LODs vary widely for a given element, reflecting the sensitivity of detection to sample composition and thickness and the presence of and interferences arising from other elements in the matrix. For most elements, and within a given category, LODs span one or two orders of magnitude among the samples. With respect to the different material categories, and based on median values, LODs are higher in foams than in plastics and ropes, presumably because of the greater contribution of air in the former (air promotes multilateral reflections and inhibits fluorescent x-rays from reaching the detector [13]). Painted surfaces exhibit the lowest LODs, likely because samples in this category contained fewer elements and lower concentrations of Cl as potential interferents (attenuating or enhancing secondary x-rays). Among the elements, LODs were generally lowest, and below 40 $\mu g\ g^{-1}$ for each category of material, for As, Br, Cr and Pb, and highest, and above 70 $\mu g\ g^{-1}$ for each category, for Ba and Cl.

3.3. Thickness correction and reference materials

Table 2 shows the results of multiple analyses (n = 5) of two reference materials manufactured by Niton (PN 180-554, batch SN PE-071-N, and PN 180-619, LOT#T-18); these are polyethylene discs of 31 mm in diameter impregnated with various elements and whose thicknesses (d ~ 13 mm) are above the saturation level for the material. Thus, without thickness correction, the FP-XRF delivers concentrations that are usually within 10% of the respective reference values; for comparison, an 'acceptable' difference from certified values of $\pm$ 20% for each analyte is stipulated by the US Environmental Protection Agency (EPA) [14]. Also shown in Table 2 are

results of analyses of a 3.4 mm section of PN 180-619 with appropriate thickness correction applied. Measured concentrations are within 12% of corresponding concentrations returned by analysis of the whole disc without thickness correction with the exception of Ba, whose measured concentration in the section was 40% greater than that in the whole disc.

Figure 1 illustrates the effect of varying the thickness correction on the concentrations returned, and after normalisation to the measured concentrations without thickness correction (and as annotated), for reference material PN 180-554; these results illustrate how different elements respond to the corrective algorithm in polyethylene. Thus, for Cr and to a lesser extent Hg, adjusting thickness correction towards its lower limit of 0.05 mm results in progressively lower normalised concentrations, while for Cd the same adjustments result in a progressively higher concentrations; normalised concentrations of Br and Pb, on the other hand, exhibit relatively little dependence on the magnitude of the thickness correction applied. Despite different concentrations of several elements being returned that were dependent on the thickness correction applied, relative error did not display any clear dependence on this variable.

3.4. Thickness correction and plastic litter

Figure 2 exemplifies the effects of applying different thickness corrections to four plastic (polyethylene and polypropylene) samples of varying size, colour, condition-age and elemental composition and where $d < d_{sat}$. Here, a wider range of elements detected are normalised to the corresponding concentrations measured after applying correction for the measured thickness, and whose values are annotated on each panel. For a given element, the precise effects and trends are different, both among the

samples and from the reference material (Figure 1), presumably because of the interactive effects that the presence of additional elements have on each other in more complex materials and the consequent corrections applied by fundamental parameters. In general, however, and with adjustments in thickness correction towards the lower limit, Ba and Sb are subject to a significant increase in normalised concentration while Cl, Cu, Fe, Ti and Zn exhibit a decrease in normalised concentration. Chlorine exhibited the greatest dependency on thickness correction in respect of the latter, and among the samples Cu, Fe and Zn exhibited a dependency whose significance appeared to exhibit an inverse dependency on the measured concentration with appropriate correction applied. Bromine, Cd, Pb and Se exhibited a dependency on thickness correction that was relatively small, with concentration differences across the range of corrections that varied by no more than 20%. As with the reference materials, relative errors did not display any clear dependence on thickness correction, but were inversely related to the absolute concentration of the element in the sample.

3.5. Thickness correction and foam and rope litter

Figure 3 shows the effects of applying different thickness corrections to six different samples containing air within their structures; namely, an expanded polystyrene, two expanded, rigid polyurethanes, a Nylon fishing line that had been intertwined and secured between two crocodile clips, a fragment of cork and on offcut of multi-coloured rope. Because d_{sat} is unknown and, likely, highly variable among such samples, sub-saturation was assumed in all cases. Thus, as above, the concentrations of different elements detected are normalised to the corresponding concentrations measured after applying correction for the measured thickness, and whose values are annotated on each panel. The findings are broadly consistent with those ascertained

371 from analyses of the plastics (Figure 2) in that adjustments in thickness correction
372 towards the lower limit of 0.05 mm are accompanied by an increase in normalised
373 concentration of Ba (note that Sb was not detected in these samples) and a reduction
374 in normalised concentration for all other elements detected. The latter effect was most
375 significant for Cl, Fe and Zn and least evident for Br and Pb, and, for the cork and two
376 of the expanded polymers, was always most pronounced at thickness corrections
377 below 2-6 mm such that trends were approximately asymptotic to unit value.
378
379 *3.6. Measurement precision and sample heterogeneity*
380 Regular assessment of precision is recommended by the US EPA [14] when using FP-
381 XRF as an important component of quality control considerations. The precision of
382 concentrations delivered by the Niton XL3t 950 He GOLDD+ on beached marine
383 litter was ascertained on a wide range of samples, in terms of material category, size,
384 thickness, colour, condition and elemental content, that were fixed in position relative
385 to the detector and measured repeatedly (n = 4 to 6) with appropriate thickness
386 correction. Precision was defined as the relative standard deviation (as a percentage)
387 arising from the repeat measurements of each sample, and results are shown in Table
388 3. Precision was highly variable, both among the different elements and between the
389 different material categories, but in all cases was better than 30% and in most cases
390 better than 20%, a recognised ‘acceptable’ objective for FP-XRF measurements [15].
391 Precision displayed a dependency on absolute concentrations (i.e. measurements of
392 higher elemental concentrations were more precise) and was also dependent on the
393 characteristics of the sample; specifically, measurements were most precise for
394 relatively thick, dense and homogeneous materials and least precise for thin,
395 expanded-extruded and more heterogeneous items.

When the same sample of plastic was located in different positions or with different orientations above the detector, repeat measurements became more variable, reflecting the different response of the detector to variations in geometry and thickness and to inherent variability in the composition and surface conditions of the polymer. Samples composed of regions of visibly different colour or texture or with areas of obvious discolouration, and in particular those in the foams and painted surfaces categories, often exhibited considerable variations in elemental concentrations that reflected significant compositional changes and/or heterogeneous contamination. Figure 4 exemplifies the spatial, surface variability of various elements on a piece of painted fibreglass backed with resin that appeared to have been derived from a boat, while Figure 5 illustrates both the surface and depth distribution of different elements in a fragment of cork that had evidently been treated or contaminated. Note an order of magnitude difference in concentrations of Bi, Cl and Pb among the different colours of paint and two orders of magnitude differences in Fe and Zn concentrations in the different regions of cork.

3.7. Summary of elemental concentrations in marine litter

Table 4 summarises the concentrations of the elements that were detected in each material category of beached marine litter, with appropriate thickness correction applied. Note that the lowest concentrations reported here for some elements are lower than minimum LODs given in Table 1 because detection is dependent on the precise composition and thickness of the sample and the presence of interfering elements; thus, for example, what may not be detected in one sample may be detected at a lower concentration in another sample which is thicker, denser and ‘cleaner’.

Note also that, in the case of As, overlap of its K_α fluorescence peak with the L_α peak of Pb and the relatively low intensity of the As-K_β line means that As concentrations cannot be effectively calculated for samples with Pb:As ratios in excess of about 10 [14]. Because false positives may often be returned for the metalloid by FP-XRF in the presence of Pb [16], As concentrations given in Table 4 are restricted to those returned where Pb was not detectable.

In the plastics category, all elements were detected, albeit in less than ten cases for As, Bi, Cd, Hg, Sb, Se, Sn and Ni. Among the remaining elements, concentrations spanned at least an order of magnitude, and in the case of Cl, Fe, Pb, Ti and Zn, at least three orders of magnitude. Regarding Cl, two samples whose concentrations exceeded 350,000 μg g^{-1} (or 35% by weight) were returned as PVC by the XRF, an identification that was confirmed by subsequent FTIR analysis. Bismuth, Cd, Hg and Se were never detected in the foams but many of the remaining elements returned a higher number (and proportion) of detectable cases in this category compared with the plastics. For example, Br, Pb and Sn were detectable in about 15, 13 and 2% of plastic samples compared with respective percentages of 75, 20 and 14%, of foam samples. Median concentrations were about an order of magnitude greater in foams than in plastics for Br, Cr, Fe and Zn; for Cl, the difference was more than two orders of magnitude and 35 samples were returned with concentrations in excess of 150,000 μg g^{-1} (or 15% by weight) and identified as PVC by the XRF. Clearly, many of these samples were not PVC-based (most of those analysed by FTIR were identified as expanded-extruded polystyrene or polyurethane) but such a classification based on a high chlorine content is a practical requirement for the appropriate fundamental parameter coefficients to be applied.

In the ropes category, Ba, Bi, Cd, Hg, Sb and Se were never detected and median concentrations of Ni and Pb were higher and Br and Zn lower than the respective median concentrations in both plastics and foams; however, compared with the latter categories, concentrations of most detectable elements in ropes encompassed considerably lower ranges in concentrations. Analysis of the painted surfaces returned no detectable Cd, Cr, Ni, Sb, Se, Sn and As and median concentrations of Ba and Ti that were higher and Cl, Cu and Fe lower than respective median concentrations in the plastics, foams and ropes categories. With the exception of Pb and Zn, the range of elemental concentrations in the painted surfaces was lower than in any of the remaining categories. Overall, and for all categories, Cl, Fe and Ti were detected in the most (> 300) and Hg and Se in the least (≤ 3) number of cases; maximum concentrations exceeded 10,000 μg g^{-1} (or 1% by weight) for Ba, Br, Cl, Fe, Pb, Ti and Zn but were never greater than 500 μg g^{-1} for Bi and Hg.

3.8. Independent analysis of marine litter by ICP following acid digestion

As an independent measure of the elemental content of beached litter, selected samples were analysed for all elements except Br and Cl by ICP-OES following H_2SO_4-HNO_3 digestion. Samples encompassed a variety of plastic fragments, expanded polymers (including polyurethane and polystyrene), ropes and a piece of cork but excluded painted surfaces. (Note that while paints could not be completely isolated from their substrates, a comparison of discrete paint fragment analysis by FP-XRF and ICP given elsewhere reveals good agreement between the two approaches [16].) The results of the present study revealed no false negatives among the samples and for all elements considered; that is, lack of detection by the XRF was not

accompanied by a measurement by ICP that exceeded the corresponding LOD of the XRF. Excluding the impacts of Pb on the detection of As by XRF (see above), false positives were returned in three cases for Cr (two plastic fragments and a piece of polystyrene foam); thus, here, the XRF reported concentrations of Cr (albeit less than 100 $\mu g\ g^{-1}$) in samples that failed to return a measurement by the more sensitive ICP-OES.

Concentrations of various elements detected by both approaches are compared in Figure 6 and statistical summaries for the data and for individual elements are shown in Table 5. Correlation analysis revealed significant relationships between [XRF] and [ICP] for all elements with the exception of Ba, and slopes, when forced through the origin, of less than 1.4 with the exception of Cu (about 8), Sn (4) and Zn (2.5) (exclusion of two expanded samples resulted in a reduction of the Cu and Zn slopes to 2.5 and 1.8, respectively). Despite most slopes being greater than 1, however, or the XRF on average returning concentrations greater than those delivered by the ICP, the relationship defining the data overall and forced through the origin ($y = 0.850x$; $r = 0.775$; $p < 0.01$; $n = 89$) indicates a slope below unit value. This discrepancy may be attributed to the weighting placed on the two data points defining the highest concentrations of Fe; thus, neglecting these points results in a slope of 1.24 ($r = 0.858$; $p < 0.01$; $n = 91$).

Given that FP-XRF provides a measurement of the elemental content at a particular location on the sample whereas ICP involves complete destruction of a sample (that likely displays some degree of heterogeneity), coupled with possible incomplete digestion of some samples on acid treatment and the presence of precipitate in other

cases, the two approaches could be considered as providing more than acceptable agreement overall according to EPA criteria [14]. Based on the results for individual elements, the quantitative performance of the XRF appears to be considerably better for elements like Cd, Pb, Sb and Se than for Cu, Sn and Zn, and in particular in expanded-extruded materials where accurate thickness correction is critical.

3.8. Advantages and limitations of FP-XRF for the analysis of marine litter

FP-XRF affords a cost-effective, non-destructive means of measuring elements in a variety of materials sampled from the pool of litter washed up on beaches, including plastics and rubbers, synthetic foams, corks, painted surfaces, ropes, fabrics and netting. With respect to the Niton XL3t 950 He GOLDD+, because it does not employ a radioactive source for the excitation of samples, training, usage and transport are not constrained by additional safety considerations and licensing and its excitation source is not subject to regular replacement. In the plastics mode, the instrument is able to analyse samples with very little preparation down to a few mg in weight and less than 3 mm in diameter, including plastic production pellets, individual spheres of expanded polystyrene, and small fragments of (micro)plastic, foam and rope, with a minimum LOD of less than 10 $\mu g\ g^{-1}$ and a precision of better than 10% in many cases. The instrument is particularly useful for measuring the spatial and depth distributions of elements in larger items and on heterogeneous surfaces which exhibit variable degrees of contamination.

Although samples whose thickness is greater than saturation are preferable in that the analysis is more sensitive and returns relatively low counting errors, an algorithm in the plastics mode is able to correct for measurements made on thinner samples in

most cases. While sample thickness has a relatively small impact on concentrations returned for some elements, like Br, Pb and Se, it has a significant impact on measurements of others, including Ba, Cl, Cr, Cu, Ti and Zn, and particularly in materials containing air, like expanded-extruded polymers and ropes, and whose thickness is below a few mm. It is critical, therefore, to apply the corrective algorithm if the latter elements are considered in samples comprised of low density materials and where $d << d_{sat}$.

An additional advantage of FP-XRF, and which has been reported in practice in the literature, is the ability to test beach litter samples in situ [9]. Pilot studies undertaken with the Niton XL3t 950 He GOLDD+ on one beach involved activating the instrument through the touch screen display in order to measure samples in contact with or in close proximity to the detector window and that had been temporarily fixed to a white plastic tray using adhesive putty. While this approach proved useful for the relatively rapid screening of some elements and the approximate abundance of others, detection limits and counting errors were relatively high and precision relatively low. This is because of the shorter counting time employed in our pilot study (20 seconds each in the main and low energy ranges), hand-held vibrations of the XRF nose and inconsistent positioning of samples in front of the detector window.

In situ application of the FP-XRF was also subject to practical difficulties associated with accurately measuring sample thickness, cleaning, drying and cutting-folding samples, orientating the flattest surface towards the detector, and measuring samples smaller than the diameter of the measurement window (i.e. < 8 mm); for a single operator of the instrument, these difficulties had a significant impact on the

546 throughput of samples. Safety was an additional concern since the analysis of
547 irregular surfaces or shapes of low density tends to create excess secondary (back
548 scattered and fluorescent) radiation. Given these constraints and considerations, and
549 our requirements for weighing, archiving and additional testing, a laboratory approach
550 involving a customised stand is recommended for the more accurate and systematic
551 characterisation of beached marine litter.
552
553 From an environmental perspective, the most important finding of the present study
554 was the occurrence and elevated concentrations of hazardous elements in many
555 samples and from all material categories considered. Most significant in this respect
556 are the heavy metals, Cd and Pb, at concentrations in excess of 1000 $\mu g\ g^{-1}$ in various
557 plastics objects and fragments, Pb and Br (the latter a component of brominated flame
558 retardants) up to concentrations of 2% in expanded-extruded polymers, and Pb at
559 concentrations of several thousand $\mu g\ g^{-1}$ in fragments of rope, netting and processed
560 cork and in paint used on wood and fibreglass. The mobilities and bioaccessibilities of
561 these elements are important considerations for risk assessment and management
562 purposes and are the subject of ongoing research.
563

564 **Acknowledgements**

565 We are grateful to Dr Andy Fisher, UoP, for performing the digests of the litter
566 samples, and Dr Ken Grainger, Niton UK, for discussions and advice relating to the
567 XRF analyses. This study was funded partly by a UoP Marine Institute grant.
568

569 **References**

570 [8] K. Ashton, L. Holmes, A. Turner, Association of metals with plastic production
571 pellets in the marine environment, Mar. Pollut. Bull. 60 (2010) 2050-2055.
572
573 [11] G.L. Bosco, Development and application of portable, hand-held X-ray
574 fluorescence spectrometers, Trend. Anal. Chem. 45 (2013) 121-134.
575
576 [4] S. Endo, R. Takizawa, K. Okuda, H. Takada, K. Chiba, H. Kanehiro, H. Ogi, R.
577 Yamashita, Concentration of polychlorinated biphenyls (PCBs) in beached resin
578 pellets: Variability among individual particles and regional differences, Mar. Pollut.
579 Bull. 50 (2005) 1103-1114.
580
581 [14] Environmental Protection Agency, Method 6200 - Field portable x-ray
582 fluorescence spectrometry for the determination of elemental concentrations in soil
583 and sediment (2007).
584 http://www3.epa.gov/epawaste/hazard/testmethods/sw846/pdfs/6200.pdf
585 Accessed 12/15.
586
587 [5] J.P.G.L. Frias, P. Sobral, A.M. Ferreira, Organic pollutants in microplastics from
588 two beaches of the Portuguese coast, Mar. Pollut. Bullet. 60 (2010) 1988-1992.
589
590 [6] J. Gauquie, L. Devrese, J. Robbens, B. De Witte, A qualitative screening and
591 quantitative measurement of organic contaminants on different types of marine plastic
592 debris, Chemosphere 138 (2015) 348-356.
593

[10] E. Hansen, N.H. Nilsson, D. Lithner, C. Lassen, Hazardous substances in plastic materials, COWI and the Danish Technological Institute on behalf of The Norwegian Climate and Pollution Agency, Oslo (2010) 150 pp.

[7] L.A. Holmes, A. Turner, R.C. Thompson, Adsorption of trace metals plastic resin pellets in the marine environment, Environ. Pollut. 160 (2012) 42-48.

[15] D.J. Kalnicky, R. Singhvi, Field portable XRF analysis of environmental samples. J. Hazard. Mater. 83 (2001) 93-122.

[3] Y. Mato, T. Isobe, H. Takada, H. Kanehiro, C. Ohtake, T. Kaminuma, Plastic resin pellets as a transport medium for toxic chemicals in the marine environment, Environ. Sci. Technol. 35 (2001) 318-324.

[1] G.R. Murray, Environmental implications of plastic debris in marine settings-entanglement, ingestion, smothering, hangers-on, hitch-hiking and alien invasions, Phil. Trans. Royal Soc. Lond. B: Biol. Sci. 364 (2009) 2013-2025.

[9] E. Nakashima, A. Isobe, S. Kako, T. Itai, S. Takahashi, Quantification of toxic metals derived from macroplastic litter on Ookushi beach, Japan, Environ. Sci. Technol. 46 (2012) 10099-10105.

[12] S. Piorek, Feasibility of analysis and screening of plastics for heavy metals with portable x-ray fluorescence analyser with miniature x-ray tube, GPEC 2004 Paper abstract #14 (2004).

[13] M. Schlummer, J. Vogelsang, D. Fiedler, L. Gruber, G. Wolz, Rapid identification of PS foam wastes containing HBCDD or its alternative PolyFR by x-ray fluorescence spectroscopy (XRF), Waste Manag. Res. (2015) doi:10.1177/0734242X15589783

[2] K. Tanaka, H. Takada, R. Yamashita, K. Mizukawa, M. Fukuwaka, Y. Watanuki, Facilitated leaching of additive-derived PBDEs from plastic by seabirds' stomach oil and accumulation in tissues. Environ. Sci. Technol. 49 (2015) 11799-11807.

[16] A. Turner, S. Comber, A.B. Rees, D. Gkiokas, K. Solman, Metals in boat paint fragments from slipways, repair facilities and abandoned vessels: an evaluation using portable XRF, Talanta 131 (2014) 372-378.

Table 1: Median, minimum and maximum limit of detection (LOD, μg g^{-1}) for each element and in the four categories of litter for a total counting time of 120 seconds and with appropriate thickness correction applied. Also shown are the numbers and percentages of cases where elements were not detected in each category and which were used to quantify the LODs. *Original res version in Excel file.*

	plastics (*n* =149)					foams (*n* = 149)					ropes (*n* = 68)					painted surfaces (*n* = 10)				
	n < LOD	% < LOD	median	min	max	*n* < LOD	% < LOD	median	min	max	*n* < LOD	% < LOD	median	min	max	*n* < LOD	% < LOD	median	min	max
As	143	96.0	3.4	1.8	231	138	92.6	23	2.9	420	59	86.8	5.6	2.3	47	6	60	1.5	1.5	1.9
Ba	132	88.6	492	217	2011	140	94.0	498	185	1734	68	100	468	281	912	8	80	384	342	454
Bi	145	97.3	12	5.5	66	149	100	49	7.1	361	68	100	17	8.4	79	9	90	5.3	3.9	72
Br	126	84.6	6.7	2.9	30	37	24.8	36	9.9	75	36	52.9	7.7	4.6	21	3	30	14	1.8	14
Cd	144	96.6	52	25	147	149	100	57	22	197	68	100	53	33	104	10	100	28	24	38
Cl	22	14.8	100	19	260	6	4.0	1233	468	1788	5	7.4	341	81	459	0	0			
Cr	72	48.3	14	2.7	46	41	27.5	35	8.7	305	36	52.9	14	4.9	31	10	100	1.5	1.5	1.7
Cu	114	76.5	24	7.9	123	120	80.5	145	17	562	21	30.9	34	21	100	8	80	6.0	3.8	16
Fe	28	18.8	25	15	56	1	0.7	625	625	625	1	1.5	56	56	56	0	0			
Hg	148	99.3	13	6.0	109	149	100	68	8.7	287	68	100	15	9.2	48	8	80	3.8	2.8	12
Ni	146	97.9	20	8.4	173	147	98.7	142	21	544	66	97.1	31	20	102	10	100	6.0	4.9	10
Pb	130	87.2	7.3	3.4	47	120	80.5	30	12.0	98	40	58.8	9.1	5.4	25	4	40	2.8	2.5	3.8
Sb	144	96.6	85	31	243	145	97.3	85	34	326	68	100	82	51	160	10	100	57	47	77
Se	147	98.7	11	4.8	126	149	100	45	6.0	215	68	100	11	7.0	34	10	100	3.5	2.6	14
Sn	146	98.0	72	34	221	127	85.2	76	26	275	67	98.5	73	44	133	10	100	37	24	38
Ti	13	8.7	8.9	2.5	28	6	4.0	314	95	1768	1	1.5	16	16	16	0	0			
Zn	76	51.0	12	6.4	36	60	40.3	91	17	238	40	58.8	15	10	34	3	30	6.1	5.1	6.4

Table 2: A comparison of reference and measured concentrations (μg g^{-1}) in two polyethylene discs supplied by Niton and that had been impregnated with various elements. Note that reference concentrations are given with estimates of errors at the 95% confidence level arising from an unspecified number of analyses while measured concentrations are shown as the mean with one standard deviation (n = 5). *Original res version in Excel file.*

material	As	Ba	Br	Cd	Cr	Hg	Pb	Sb	Se
PN 180-554									
reference			495±20	150±6	995±40	1000±40	1002±40		
measured with no thickness correction			497±3	135±5	1060±7	912±5	964±21		
PN 180-619									
reference	51±7	704±45		292±20	106±10	101±10	155±12	94±10	207±15
measured with no thickness correction	46±2	761±25		295±5	116±8	93±3	136±2	98±3	228±4
PN 180-619: 3.4 mm section									
measured with thickness correction	44±4	1060±130		319±12	124±2	82±5	138±7	109±19	209±5

Table 3: Number of cases detected and median, minimum and maximum precisions (as % relative standard deviation) for each element and in the four categories of litter for a total counting time of 120 seconds and with appropriate thickness correction applied. *Original res version in Excel file.*

	plastics (*n* =6)				foams (*n* = 5)				ropes (*n* = 3)				painted surfaces (*n* = 6)			
	n > LOD	median	min	max	*n* > LOD	median	min	max	*n* > LOD	median	min	max	*n* > LOD	median	min	max
As	4	14.2	6.0	24.6	2	12.0	10.5	13.5	3	13.0	10.6	21.1	4	5.2	0.6	19.9
Ba	2	10.4	3.1	17.7	0				0				2	4.8	1.3	8.3
Bi	0				0				0				1	24.6	24.6	24.6
Br	0				5	4.5	1.5	12.0	1	1.3	1.3	1.3	3	4.8	1.1	10.6
Cd	3	1.6	0.6	7.9	0				0				0			
Cl	5	5.9	3.1	11.5	5	1.6	0.6	4.3	3	6.4	2.9	7.5	6	2.7	0.1	17.0
Cr	6	3.9	1.1	13.8	4	4.7	4.0	7.9	3	2.3	1.5	2.5	0			
Cu	1	16.5	16.5	16.5	4	13.8	9	21.8	1	7.5	7.5	7.5	0			
Fe	5	3.1	1.2	8.8	5	3.6	0.8	11.1	3	4.0	0.8	18.2	6	3.7	0.1	4.7
Hg	0				0				0				0			
Ni	2	17.6	15.9	19.4	0				0				0			
Pb	4	1.7	0.9	4.3	2	4.0	3.1	4.8	3	2.6	1.3	3.6	5	2.0	0.4	16.5
Sb	3	9.8	2.3	18.4	0				2	21.7	17.8	25.5	0			
Se	1	2.9	2.9	2.9	0				0				0			
Sn	0				2	12.6	8.7	16.5	0				0			
Ti	6	2.6	0.6	10.8	5	8.7	1.5	21.2	2	2.5	2.5	2.5	6	0.9	0.5	6.4
Zn	6	4.7	2.0	14.2	4	7.7	5.6	10.0	1	15.7	15.7	15.7	6	3.1	1.1	7.7

Table 4: Number of cases detected and median, minimum and maximum concentrations (μg g^{-1}) for each element and in the four categories of litter for a total counting time of 120 seconds and with appropriate thickness correction applied. *Original res version in Excel file.*

	plastics (*n* =149)				foams (*n* = 149)				ropes (*n* = 68)				painted surfaces (*n* = 10)			
	n > LOD	median	min	max	*n* > LOD	median	min	max	*n* > LOD	median	min	max	*n* > LOD	median	min	max
As	1	6.2	6.2	6.2	9	56	25	210	2	27	17	36	0			
Ba	17	1710	329	10,700	9	1090	298	20,400	0				2	4070	4030	4100
Bi	4	88	20	198	0				0				1	79	79	79
Br	23	32	4.8	1180	112	218	12	17,600	32	20	6.6	91	7	37	5.6	61
Cd	5	1940	117	4640	0				0				0			
Cl	127	594	4.3	408,000	143	60,700	744	572,000	63	958	189	20,400	10	39	9.6	614
Cr	77	34	21	717	108	210	23	940	32	63	25	909	0			
Cu	35	60	22	718	29	203	71	1910	47	76	27	808	2	14.0	10	18
Fe	121	136	20	28,700	148	7570	279	120,000	67	1160	88	29,200	10	90	11	400
Hg	1	272	272	272	0				0				2	7.3	4.0	11
Ni	3	29	19	74	2	220	220	220	2	386	37	735	0			
Pb	19	58	6.3	13,200	29	119	6.7	17,000	28	199	13	3770	6	175	3.6	10,700
Sb	5	228	154	6260	4	259	67	5819	0				0			
Se	2	457	351	563	0				0				0			
Sn	3	486	35	2090	22	209	53	2280	1	83	83	83	0			
Ti	136	387	5.6	63,900	143	867	18	30,400	67	386	16.8	3140	10	2920	3.5	454
Zn	73	39	13	26,700	89	229	25	25,300	28	30	15	535	7	92	6.0	1570

Table 5: Parameters defining the relationships between FP-XRF and ICP-OES measurements of various marine litter samples. The slope, *m*, correlation coefficient (significant at $p < 0.01$), *r*, and number of data points, *n*, are shown for each element and, for Cu and Zn (and in parentheses), after exclusion of two foam samples. *Original res version in Excel file.*

element	*m*	*r*	*n*
Ba	1.48*	ns	4
Cd	1.05	0.969	4
Cr	1.33	0.550	12
Cu	8.02 (1.72)	0.849 (0.871)	7 (5)
Fe	0.75	0.948	15
Pb	1.39	0.795	11
Sb	1.34	0.999	3
Se	1.18	0.999	2
Sn	4.03	0.997	3
Ti	1.17	0.984	18
Zn	2.54 (1.59)	0.641 (0.999)	12 (10)

*Since the relationship for Ba was not significant, the slope is represented as the average ratio defining the concentrations derived from the two approaches.

Figure 1: Elemental concentrations in the reference polyethylene disc, PN-180-554, as a function of thickness correction applied and for a total counting time of 120 seconds. Note that concentrations are normalised to values shown in the legend (in μg g^{-1} and derived without thickness correction). *High res version in Excel file.*

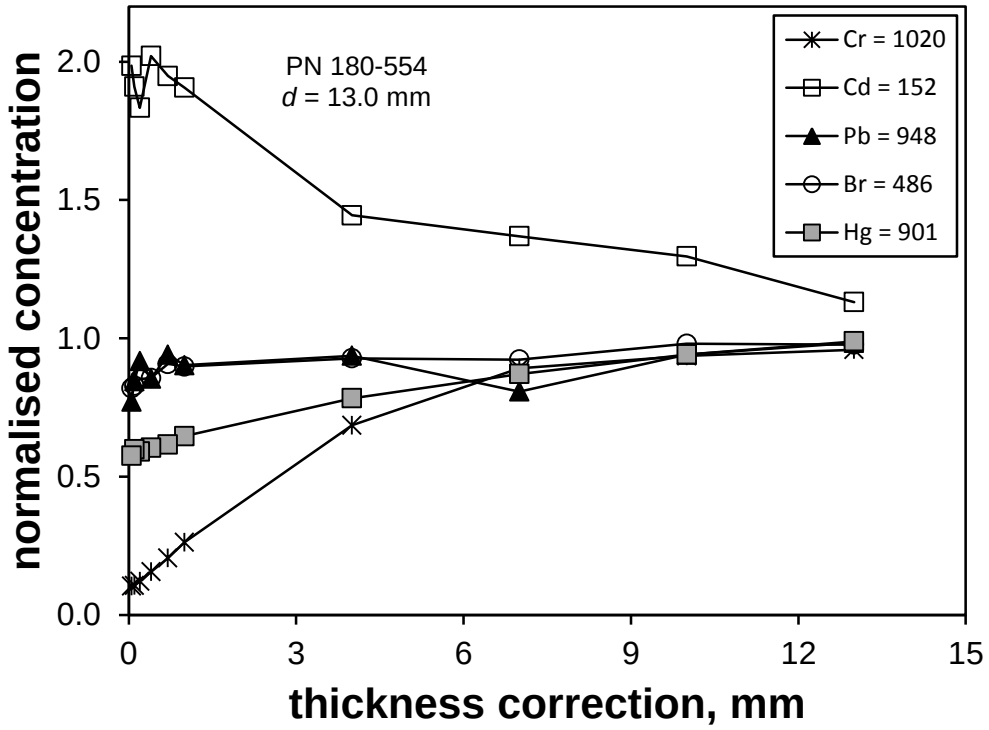

Figure 2: Elemental concentrations in various plastic (polyethylene and polypropylene) litter samples as a function of thickness correction applied and for a total counting time of 120 seconds. Note that concentrations are normalised to values shown in the legend (in μg g^{-1} and derived with appropriate thickness correction). *High res version in Excel file.*

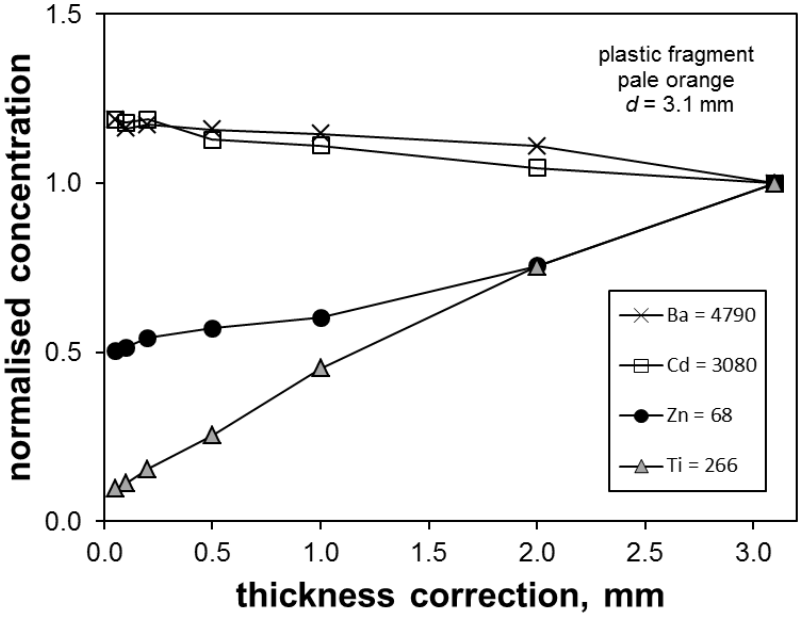
plastic fragment
pale orange
d = 3.1 mm
Ba = 4790
Cd = 3080
Zn = 68
Ti = 266
normalised concentration
thickness correction, mm
0.0
0.5
1.0
1.5
2.0
2.5
3.0

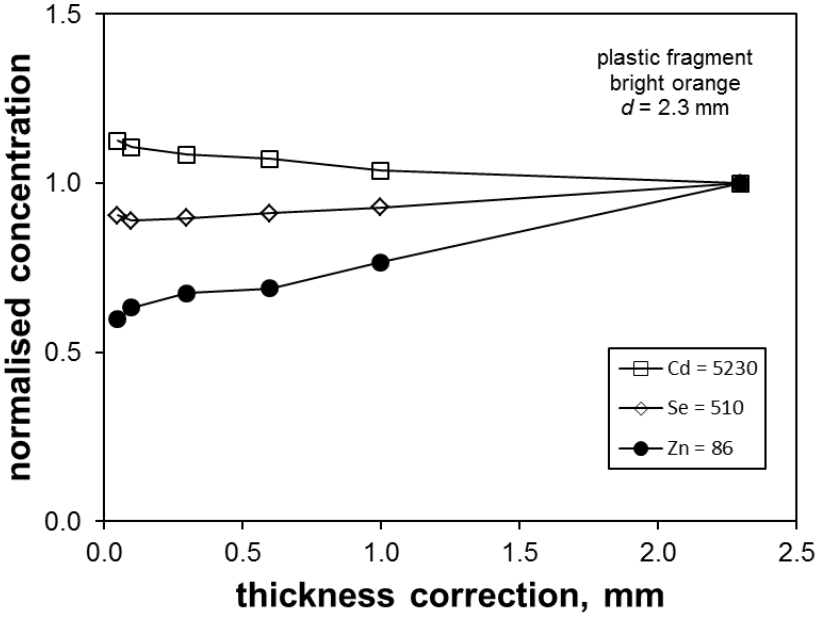
plastic fragment
bright orange
d = 2.3 mm
Cd = 5230
Se = 510
Zn = 86
normalised concentration
thickness correction, mm
0.0
0.5
1.0
1.5
2.0
2.5

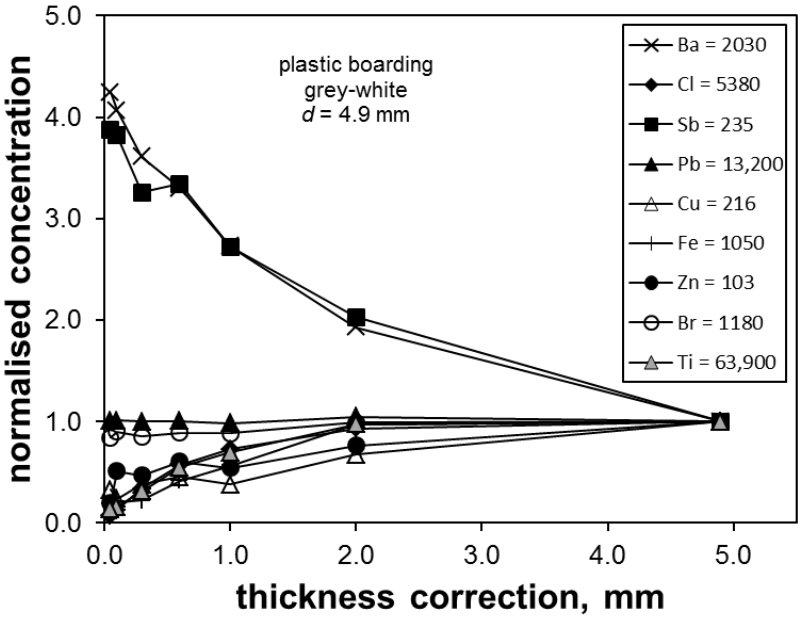
plastic boarding
grey-white
d = 4.9 mm
Ba = 2030
Cl = 5380
Sb = 235
Pb = 13,200
Cu = 216
Fe = 1050
Zn = 103
Br = 1180
Ti = 63,900
normalised concentration
thickness correction, mm
0.0
1.0
2.0
3.0
4.0
5.0

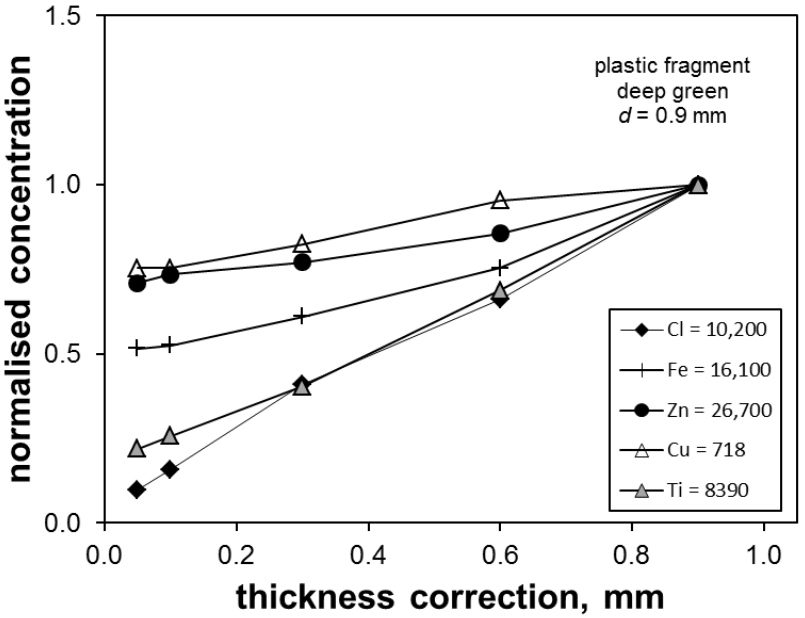
plastic fragment
deep green
d = 0.9 mm
Cl = 10,200
Fe = 16,100
Zn = 26,700
Cu = 718
Ti = 8390
normalised concentration
thickness correction, mm
0.0
0.2
0.4
0.6
0.8
1.0
0.5
1.0
1.5

Figure 3: Elemental concentrations in various foams (including a fragment of cork) and ropes as a function of thickness correction applied and for a total counting time of 120 seconds. Note that concentrations are normalised to values shown in the legend (in μg g^{-1} and derived with appropriate thickness correction). EPS = expanded polystyrene; EPU = expanded polyurethane. *High res version in Excel file.*

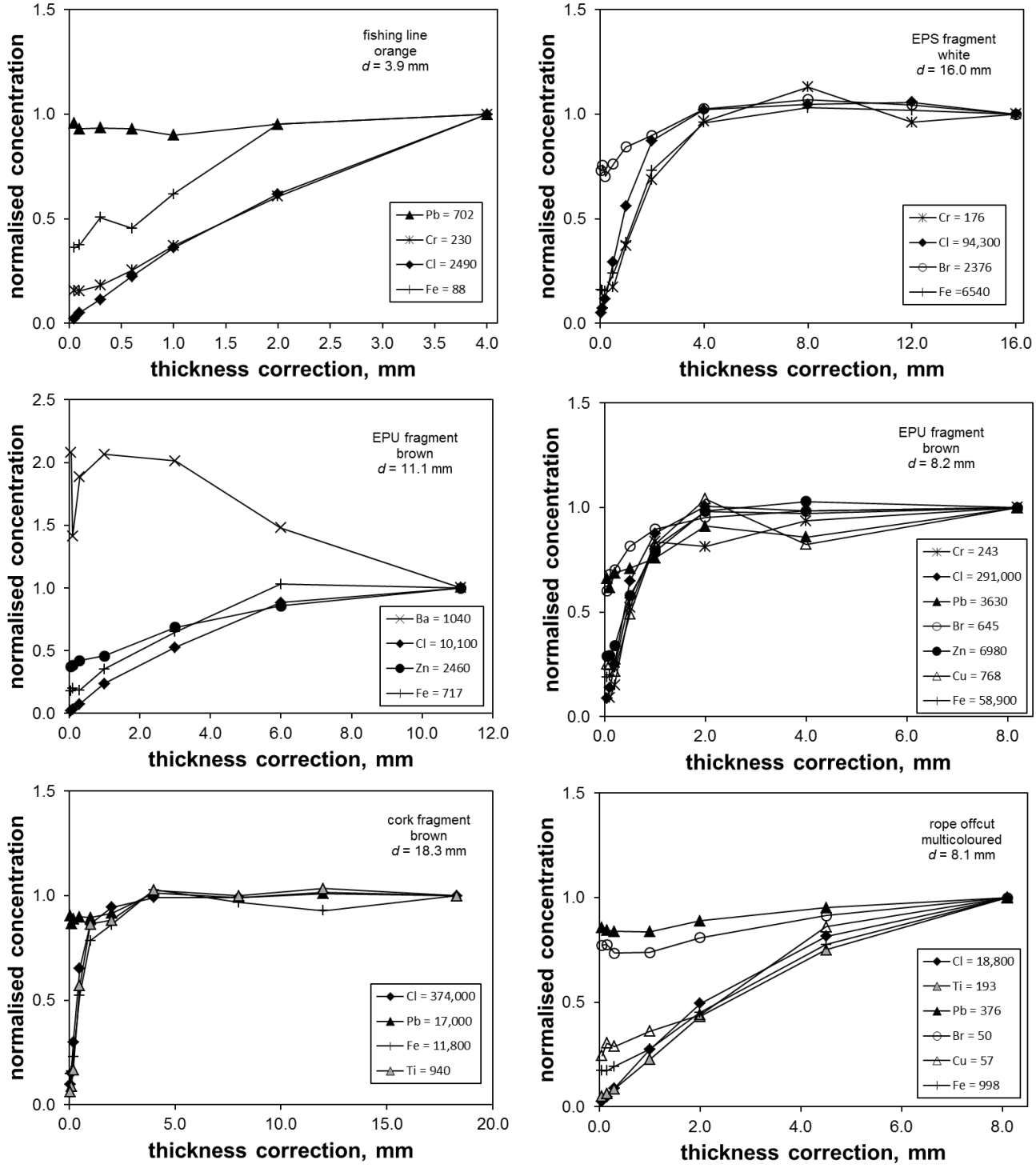

Figure 4: Spatial distribution of various elements (in μg g^{-1}) measured at the surface of a fragment of painted acrylic-fibreglass with resinous backing. *(for colour reproduction on the web)*

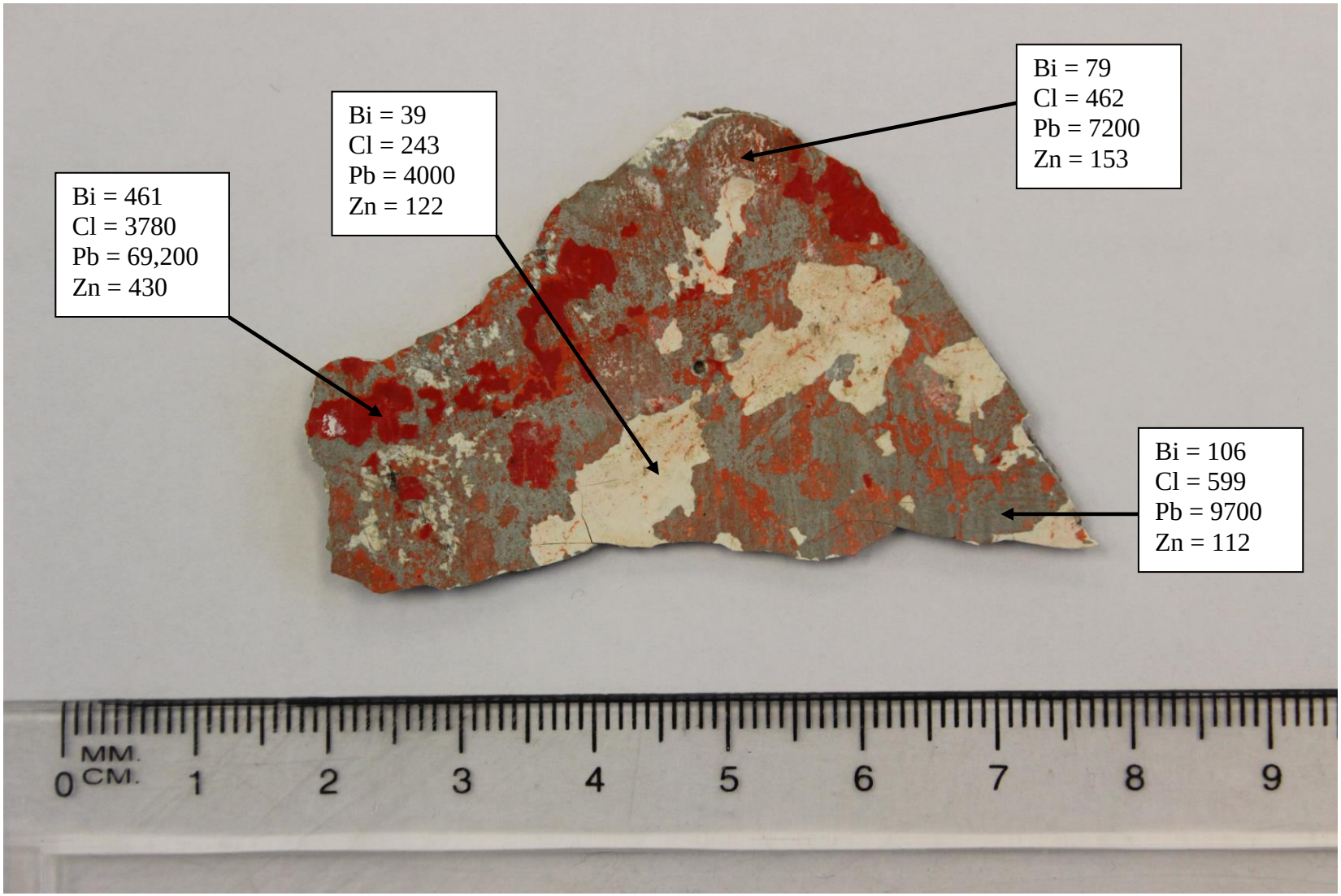

Figure 5: Spatial and depth distribution of various elements (in μg g^{-1}) in a fragment of cork that had been sliced with a stainless steel scalpel. *(for colour reproduction on the web)*

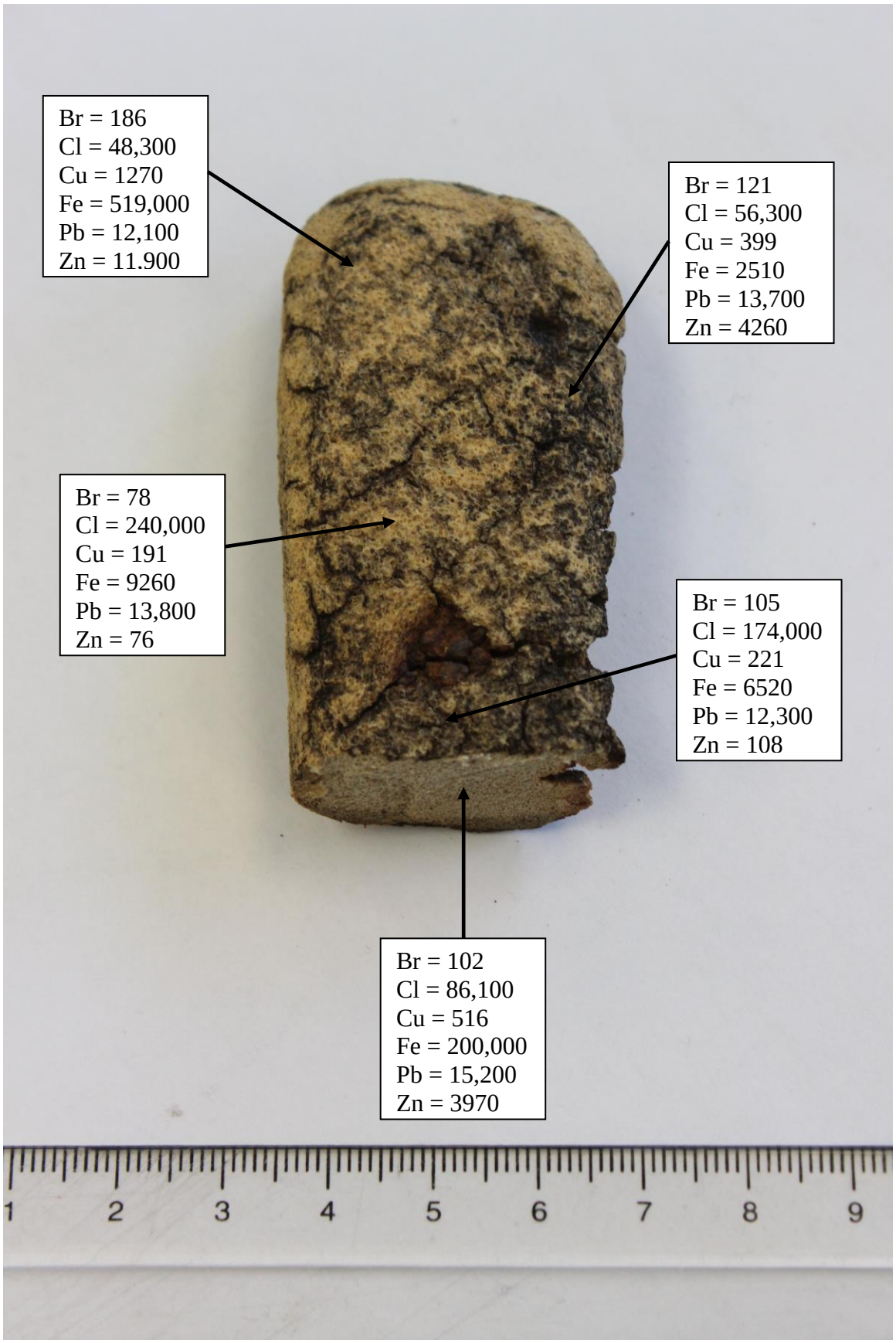

Figure 6: A comparison of the concentrations of elements in various samples of marine litter returned by the FP-XRF and by ICP-OES following acid digestion. Annotated are lines defining unit slope and ratios of [XRF] to [ICP] of 10:1 and 1:10. *High res version in Excel file.*